Available online at www.sciencedirect.com
ScienceDirect
IFAC PapersOnLine 50-1 (2017) 4492–4497

MPPT and yaw control combination of a new twin wind turbines structure

I. Guenoune. * **F. Plestan.** * **A. Chermitti** **

* *Ecole Centrale de Nantes-LS2N, 4321 Nantes, France.*
Ibrahim.Guenoune@irccyn.ec-nantes.fr
Franck.Plestan@irccyn.ec-nantes.fr.
** *LAT, Université de Tlemcen, Algérie.*
a.chermitti@yahoo.fr

Abstract: A robust integral backstepping controller is designed in this paper in order to control a new structure of twin wind turbines. The novelty of this concept is the free motion of the arms carrying the two turbines. In order to initiate a yaw rotation, the pitch blades angles are modified to create a difference between the drag forces of the two rotors. The controller aims at maximizing the electrical power by an optimal orientation of the structure. A strategy based on backstepping approach is proposed.

Keywords: Twin wind turbines, maximum power point tracking (MPPT), integral backstepping controller (IBC), yaw motion.

1. INTRODUCTION

The wind variations (speed, direction) and the uncertainties of the turbine modeling are the main reasons to design robust controllers for such systems. A non-efficient controller, which would be too much impacted by these disturbances or uncertainties, would induce a reduced level of energy production, that is not acceptable.
Several control strategies have been developed to improve the power production, alleviate the fatigue loads and reduce the cost maintenance. The control of the wind turbine, especially at below rated wind speed, aims to reach high efficiency by controlling the rotor speed in order to get a large value of the power coefficient [Beltran et al. (2009)]-[Jafarnejadsani et al. (2013)].
Indeed, as previously suggested, this efficiency is affected by the variation of wind direction. The most part of wind turbines are equipped with a rotation system in nacelle (actuator) to suppress the misalignment with the wind direction [Shariatpanah et al. (2013)]. However, this technology makes a huge nacelle system which increase the installation cost.
In this work, an integral backstepping controller is designed to control an original new structure of twin wind turbines patented by [Herskovits et al. (2014)]. The main feature of this concept is the free rotation of the arm, which carries the two identical wind turbines. It means that no additional yaw drive motor is required to rotate the entire structure face the wind.
With a variation of the pitch angles of the two wind turbines blades, around an optimal value, a difference of the aerodynamic coefficients (*i.e.* drag force) is created between the two rotors. Therefore, this difference is used to unbalance the yaw trim. The difficulty of the SEREO system is that there is no additional yaw system (motor drive), which is the novelty of this structure. Then, it is necessary to design an appropriate control strategy for the SEREO structure without yaw actuation in order to optimize the output power.
The main contributions of this work consist in designing the nonlinear robust control applied to SEREO structure. For the control part, the rotor speed of the two wind turbines is controlled by adjusting the generator torque, while the yaw rotation is controlled thanks to the pitch angles variation (drag force difference).
The rest of this work is organized as follows. In Section II, the nonlinear model of the TWT including the aerodynamic model, yaw dynamics and the model of the permanent magnet synchronous generator, is introduced. Problem formulation and control strategy are described in Section III. Then, simulation results are presented in Section IV.

2. MODELING OF THE *SEREO* STRUCTURE

The new structure of twin wind turbines [Herskovits et al. (2014)] is presented in Figure 1. The free rotation of the arms, which are carrying the two turbines, is the main novelty of this structure. It means that the two wind turbines can be face the wind without using a motor actuator, in contrast to standard wind turbines, which need an actuator to rotate the nacelle system [Shariatpanah et al. (2013)]-[Mesemanolis and Mademlis (2014)].

The control of such SEREO structure, which is displayed in the next section, must guarantee an optimal energy through the right orientation of the entire structure.

In this section, a full model of the SEREO structure [Guenoune et al. (2016)] is detailed and composed of the aerodynamic model, pitch angle dynamics, yaw dynamics, and angular velocities dynamics of the generators.

* This work is supported by EU-METALIC II Program.

2405-8963 © 2017, IFAC (International Federation of Automatic Control) Hosting by Elsevier Ltd. All rights reserved.
Peer review under responsibility of International Federation of Automatic Control.
10.1016/j.ifacol.2017.08.379

Fig. 1. SEREO structure [Herskovits et al. (2014)] composed of twin wind turbines.

2.1 Aerodynamic and mechanical model

Figure 2 shows a simplified scheme of the SEREO structure, viewed from the Top. In the rest of the paper, the turbines are denoted with an index i, such that $i \in \{1, 2\}$, which gives Turbine 1 and Turbine 2. From Figure 2, ψ (resp. α) is the orientation of the full system with respect to the True North (resp. the angle between the True North and the wind direction).

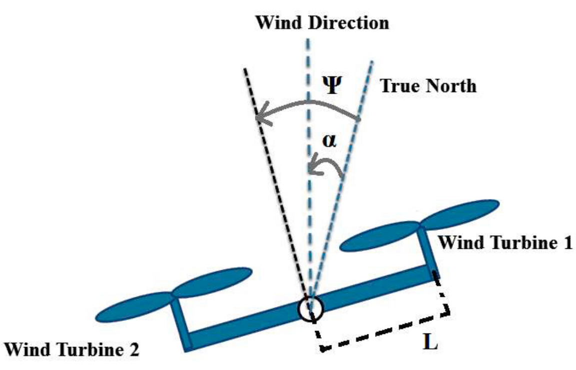

Fig. 2. Simplified model of the SEREO structure (view from the top) [Guenoune et al. (2016)]

The mechanical power P_{ai} captured by the turbine i, the aerodynamic torque Γ_{ai} and the drag force F_{di} are given by [Munteanu et al. (2008)]-[Jafarnejadsani et al. (2013)]

$$\begin{aligned} P_{ai} &= \frac{1}{2} C_{p,i}(\lambda_i, \beta_i)\, \rho\, \pi\, R^2\, (V \cos(\psi - \alpha))^3 \\ \Gamma_{ai} &= \frac{1}{2} \frac{C_{p,i}(\lambda_i, \beta_i)}{\lambda_i}\, \rho\, \pi\, R^3\, (V \cos(\psi - \alpha))^2 \\ F_{di} &= \frac{1}{2} C_{d,i}(\lambda_i, \beta_i)\, \rho\, \pi\, R^2\, (V \cos(\psi - \alpha))^2 \end{aligned} \tag{1}$$

with R the radius of the wind turbines blades, ρ the air density, V the wind velocity, β_i the pitch angle of the blades, and λ_i the tip-speed ratio (TSR). This latter parameter is defined as

$$\lambda_i = \frac{\Omega_i}{V \cos(\psi - \alpha)} R \tag{2}$$

The power coefficient $C_{p,i}$ depends on the TSR and the pitch angle [Uehara et al. (2011)], and reads as

$$C_{p,i}(\lambda_i, \beta_i) = 0.22\,(116\, a - 0.4\, \beta_i - 5)\, e^{-12.5\, a} \tag{3}$$

with

$$a = \frac{1}{\lambda_i + 0.08\, \beta_i} - \frac{0.035}{\beta_i^3 + 1},$$

The characteristics $C_{p,i} - \lambda_i$ for different values of pitch angle is displayed in Figure 3. It can be observed that there is a single pair (λ_i, β_i) for which the power coefficient has a maximum value denoted $C_{p,i}^{max}$. The control must force the two turbines to follow $C_{p,i}^{max}$ to produce the maximal power, by varying the angular velocities in order to maintain the system at the optimum speed ratio λ_i^{opt} [1] [Uehara et al. (2011)]-[Beltran et al. (2009)].

The black bold curve (AB) (Figure 3) corresponds to the maximal power coefficient with respect to the value λ_i and β_i. Along this curve, by applying the MPPT (Maximum Point Power Tracking) strategy, the turbines operate in high efficiency. Finally, this curve allows to link λ_i and an *optimal* pitch angle β_i^{opt}, which corresponds to optimal value of $C_{p,i}$: in this case, for each value of λ_i, β_i has an optimal value denoted β_i^{opt}.
In contrast to [Uehara et al. (2011)], in which the optimal pitch angle is taken constant ($\beta^{opt} = 2°$), the optimal value of pitch angle is given here by a function of λ_i [Tang et al. (2011)]

$$\begin{aligned} \beta_i^{opt} = &\; 0.0219\, \lambda_i^4 - 0.2810\, \lambda_i^3 + 0.4421\, \lambda_i^2 \\ & + 11.8415\, \lambda_i - 7.9378 \end{aligned} \tag{4}$$

The drag coefficient $C_{d,i}$ [Georg. et al. (2012)] is a

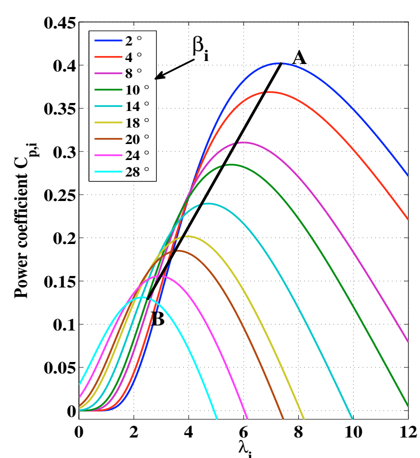

Fig. 3. Power coefficient $C_{p,i}$ versus the tip-speed ratio λ_i, for different values of pitch angle β_i.

nonlinear function of the TSR and the pitch angle. A least squares polynomial interpolation method allows to get an expression of $C_{d,i}$ that reads as

$$\begin{aligned} C_{d,i}(\lambda_i, \beta_i) = &\; \underbrace{a_0 + a_1\, \lambda_i + a_2\, \lambda_i^2 + a_3\, \lambda_i^3}_{\mathcal{A}_i} \\ & + \underbrace{\left(b_0 + b_1\; \lambda_i + b_2\; \lambda_i^2 + b_3\; \lambda_i^3\right)}_{\mathcal{B}_i} \cdot \beta_i \end{aligned} \tag{5}$$

with $a_0 = 0.25382$, $a_1 = -0.1369$, $a_2 = 0.04345$, $a_3 = -0.00263$, $b_0 = -0.008608$, $b_1 = 0.0063$, $b_2 = -0.0015$ and $b_3 = 0.000118$.

[1] λ_i^{opt} is the optimal value of the tip speed ratio.

2.2 Blade pitch dynamics

The drag forces F_{di} of the both wind turbines can be modified by changing the pitch angles β_1 and β_2, allowing to rotate the SEREO structure.
It is supposed that there is an inner loop for the control of both pitch angles, such that these both angles read as [see Guenoune et al. (2016)]

$$\begin{aligned} \beta_1 &= \beta_1^{opt} + \Delta\beta_1 \\ \beta_2 &= \beta_2^{opt} + \Delta\beta_2 \end{aligned} \tag{6}$$

with β_1^{opt}, β_2^{opt} defined from (4), $\Delta\beta_1$ and $\Delta\beta_2$ being viewed as the control inputs controlling the rotation of the structure.

2.3 Yaw dynamics

The dynamics of the rotation of the SEREO structure around its vertical axis is given by

$$K_r\ddot{\psi} = -D_r\dot{\psi} + (F_{d1} - F_{d2})\,L \tag{7}$$

with K_r the inertia moment associated to yaw motion, D_r the friction coefficient, and L the length between the horizontal axis and the vertical axis (Figure 2).
From (1)-(5), one gets

$$\begin{aligned} F_{d1} - F_{d2} &= \frac{1}{2}\rho\pi(RV\cos(\psi-\alpha))^2\,(C_{d,1} - C_{d,2}) \\ &= \frac{1}{2}\rho\pi(RV\cos(\psi-\alpha))^2\,[\mathcal{A}_1 - \mathcal{A}_2 \\ &\quad +\mathcal{B}_1\cdot\beta_1 - \mathcal{B}_2\cdot\beta_2] \end{aligned} \tag{8}$$

Define $\varphi(\psi, \beta_1, \beta_2, \lambda_1, \lambda_2)$ as

$$\varphi = \mathcal{C}\,[\mathcal{A}_1 - \mathcal{A}_2 + \mathcal{B}_1\cdot\beta_1 - \mathcal{B}_2\cdot\beta_2] \tag{9}$$

with $\mathcal{C} = \frac{1}{2}\rho\pi(RV\cos(\psi-\alpha))^2$.

2.4 Velocity dynamics of the turbines

The dynamics of the angular velocities of each generator (PMSG) is given by [Munteanu et al. (2008)]

$$\begin{aligned} J\,\dot{\Omega}_1 &= \Gamma_{a1} - \Gamma_{em1} - f_v\,\Omega_1 \\ J\,\dot{\Omega}_2 &= \Gamma_{a2} - \Gamma_{em2} - f_v\,\Omega_2 \end{aligned} \tag{10}$$

with $\Gamma_{em1,em2}$ the electromagnetic torques of the generators, J the total inertia, and f_v the friction coefficient. Note that the both electromagnetic torques will be viewed as two control inputs, allowing to control the angular velocities.

2.5 Nonlinear model of the SEREO system

Assumption 1. One supposed that $\mid \Omega_1 \mid = \mid \Omega_2 \mid$, which gives that
$\lambda_1 = \lambda_2 = \lambda$ and $\lambda_1^{opt} = \lambda_2^{opt} = \lambda^{opt}$

From (4) and if the structure is face the wind, one has $\beta_1^{opt} = \beta_2^{opt} = \beta^{opt}$, which gives

$$\begin{aligned} \beta_1 &= \beta^{opt} + \Delta\beta_1 \\ \beta_2 &= \beta^{opt} + \Delta\beta_2 \end{aligned} \tag{11}$$

From Assumption 1, equation.(9) reads as

$$\varphi = \mathcal{C}\,\mathcal{B}\cdot[\beta_1 - \beta_2] \tag{12}$$

with $\mathcal{A}_1 - \mathcal{A}_2 = 0$, $\mathcal{B}_1 = \mathcal{B}_2 = \mathcal{B}$.

Assumption 2. Given that the rotation of the structure is made through the drag forces difference created between the two rotors, one states $\Delta\beta_1 = -\Delta\beta_2 = \Delta\beta$, then

$$\begin{aligned} \beta_1 &= \beta_{opt} + \Delta\beta \\ \beta_2 &= \beta_{opt} - \Delta\beta \end{aligned} \tag{13}$$

From these assumptions, a reduced model is defined as

$$\dot{x} = f(x) + g(x)\cdot u \tag{14}$$

with $x = [\psi\ \dot{\psi}\ \Omega_1\ \Omega_2]^T$, $u = [\Delta\beta\ \Gamma_{em1}\ \Gamma_{em2}]^T$,

$$f = \begin{bmatrix} \dot{\psi} \\ \frac{-D_r}{K_r}\,\dot{\psi} \\ \frac{\Gamma_{a1}(\lambda_1, \Omega_1, V, \psi)}{J} \\ \frac{\Gamma_{a2}(\lambda_2, \Omega_2, V, \psi)}{J} \end{bmatrix}$$

$$g = \begin{bmatrix} 0 & 0 & 0 \\ \frac{L}{K_r}\,\mathcal{C}\,(\mathcal{B}_1 + \mathcal{B}_2) & 0 & 0 \\ 0 & \frac{-1}{J} & 0 \\ 0 & 0 & \frac{-1}{J} \end{bmatrix} \tag{15}$$

where $f_v = 0$ (see Uehara et al. (2011)).

3. ROBUST CONTROL STRATEGY

3.1 Problem formulation

When the wind turbines are face the wind, the control of the SEREO structure has to ensure optimal production of electrical power.
In case of a change of wind direction, the TWT must rotate to follow this variation. The standard wind turbines require an actuator to rotate the nacelle system [Shariatpanah et al. (2013)]. With SEREO structure (Figure 1), the rotation is made, with no additional actuator, but by creating a drag force difference between the two rotors. Then, two control problems have to be managed

- the first one consists in controlling the rotation velocity of each turbine, in order to get the larger value of $C_{p,i}$;
- the second one consists in ensuring that the two turbines are face the wind - it yields to ensure that the error angle $\psi - \alpha$ converges to 0, thanks to an action on the blades pitch angles β_1, β_2.

Note that when the TWT is not face the wind, the generated power is not optimal because the pitch angle is not *formally optimal*, but it is used to ensure the rotation of the structure.

Yaw rotation of the structure When the structure is oriented face the wind, there is no difference of the drag force ($F_{d1} - F_{d2} = 0$). If the wind direction changes, a yaw error appears (see Figure 2); then, the rotation of the twin wind turbines is required to track this variation. As said above, the yaw motion of the structure does not require a driven motor. Therefore, the pitch angles of the two wind turbines are changed, to create a drag force difference between the rotors. Thanks to this difference, a yawing torque Γ_ψ defined as

$$\Gamma_\psi = (F_{d1} - F_{d2})\, L \tag{16}$$

is appearing and forces the rotation.

Angular velocities control As previously explained, the two wind turbines have to reach the maximum power coefficient, by keeping their tip-speed ratios at their optimal values. Therefore, the angular velocities are controlled at a same reference (*i.e.* $\Omega_1^* = \Omega_2^* = \Omega^*$), which are derived from (2), by acting on the generators electromagnetic torques. Then, the reference of the rotational speeds is derived from (2) which gives

$$\Omega^* = \frac{V\cos(\psi - \alpha)}{R}\, \lambda^{opt} \tag{17}$$

with λ_1 and λ_2 replaced by λ^{opt} to get the optimum angular velocity.

3.2 Control Strategy

The Backstepping control strategy is designed more for nonlinear systems. The idea of this method is that the closed-loop system is transformed into first order subsystems. By applying this control law, the asymptotic stability of the tracking error and the system robustness are established and checked thanks to Lyapunov approach [Glumineau and d. L. Morales (2015)].

In this proposed control design, the error tracking is modified by addition of integral terms, in order to improve the robustness of the system against perturbations and parameters uncertainties.

3.3 Control design

Speed control The tracking error of the two angular velocities is defined as

$$Z_{\Omega i} = \Omega_i^* - \Omega_i + k'_{\Omega i} \int_0^t (\Omega_i^* - \Omega_i)\,\mathrm{d}t \tag{18}$$

and its time derivative is given by

$$\dot{Z}_{\Omega i} = \dot{\Omega}_i^* - \frac{1}{J}\,\Gamma_{ai} + \frac{1}{J}\,\Gamma_{emi} + \frac{f_v}{J}\,\Omega_i + k'_{\Omega i}\,(\Omega_i^* - \Omega_i) \tag{19}$$

Choosing the Lyapunov function candidate and its derivative with respect to time as

$$V_{\Omega i} = \frac{1}{2}\, Z_{\Omega i}^2 \tag{20}$$

$$\dot{V}_{\Omega i} = Z_{\Omega i}\Big\{\dot{\Omega}_i^* - \frac{1}{J}\,\Gamma_{ai} + \frac{1}{J}\,\Gamma_{emi} + \frac{f_v}{J}\,\Omega_i + k'_i\,(\Omega_i^* - \Omega_i)\Big\} \tag{21}$$

Applying the backstepping strategy, the control inputs are chosen as

$$\Gamma_{em1} = J\Big\{ - K_{\Omega 1} Z_{\Omega 1} - \dot{\Omega}_1^* + \frac{1}{J}\,\Gamma_{a1} - \frac{f_v}{J}\,\Omega_1 - k'_{\Omega 1}\,(\Omega_1^* - \Omega_1)\Big\} \tag{22}$$

$$\Gamma_{em2} = J\Big\{ - K_{\Omega 2} Z_{\Omega 2} - \dot{\Omega}_2^* + \frac{1}{J}\,\Gamma_{a2} - \frac{f_v}{J}\,\Omega_2 - k'_{\Omega 2}\,(\Omega_2^* - \Omega_2)\Big\} \tag{23}$$

Then, one gets

$$\dot{V}_{\Omega 1} = -K_{\Omega 1} Z_{\Omega 1}^2$$
$$\dot{V}_{\Omega 2} = -K_{\Omega 2} Z_{\Omega 2}^2, \qquad K_{\Omega 1}, K_{\Omega 2} > 0.$$

Yaw angle control To maintain the alignment of the twin wind turbines with respect to the wind direction, the angle $\psi - \alpha$ must be forced at 0.

Step 1. Define the tracking error of the yaw angle as

$$Z_1 = \psi - \psi^* + k'_1 \int_0^t (\psi - \psi^*)\,\mathrm{d}t \tag{24}$$

with ψ^* the reference value of the yaw angle defined as

$$\psi^* = \begin{cases} 0 & (Structure\ face\ the\ wind) \\ \alpha & (yaw\ rotation\ \longrightarrow following\ \alpha). \end{cases}$$

Consider the candidate Lyapunov function and its time derivative as

$$V_1 = \frac{1}{2} Z_1^2 + \frac{1}{2} Z_1'^2 \tag{25}$$

$$\dot{V}_1 = Z_1\,\dot{Z}_1 + Z'_1\,\dot{Z}'_1. \tag{26}$$

By taking $\dot{Z}_1 = -K_1\, Z_1$ and $\dot{Z}'_2 = -k'_1\, Z'_1$, it follows that

$$\dot{V}_1 = -K_1\, Z_1^2 - k'_1\, Z_1'^2 \tag{27}$$

with K_1 and k'_1 are the positive constants.

Step 2. In order to design the control law $\Delta\beta$, a new tracking error is defined

$$Z_2 = \dot{\psi} - \dot{\psi}^* + k'_2 \int_0^t (\dot{\psi} - \dot{\psi}^*)\,\mathrm{d}t \tag{28}$$

Choosing the following candidate Lyapunov function

$$V_2 = V_1 + \frac{1}{2} Z_2^2 + \frac{1}{2} Z_2'^2, \tag{29}$$

the time derivative of this candidate function is given as

$$\dot{V}_2 = \dot{V}_1 + Z_2\Big\{\frac{-D_r}{K_r}\,\dot{\psi} + \frac{1}{K_r}\, 2\,L\,\mathcal{C}\,\mathcal{B}\,\Delta\beta - \ddot{\psi}^* + + k'_2(\dot{\psi} - \dot{\psi}^*)\Big\} + Z'_2\, k'_2(\dot{\psi} - \dot{\psi}^*) \tag{30}$$

Choose the control input $\Delta\beta$ as

$$\Delta\beta = \frac{K_r}{2\,L\,\mathcal{C}\,\mathcal{B}}\Big[- K_2\, Z_2 + \ddot{\psi}^* + \frac{D_r}{K_r}\,\dot{\psi} - k'_2(\dot{\psi} - \dot{\psi}^*)\Big] \tag{31}$$

By substituting (31) in (30), one has

$$\dot{V}_2 = -K_1\, Z_1^2 - k_1'\, Z_1'^2 - K_2\, Z_2^2 + \left\{ Z_2 + Z_2' \right\} k_2' \,(\dot{\psi}^* - \dot{\psi}). \tag{32}$$

Since $\dot{\psi} - \dot{\psi}^* = Z_2 - Z_2'$, then equation (32) becomes

$$\dot{V}_2 = \overbrace{-K_1\, Z_1^2 - k_1'\, Z_1'^2}^{\dot{V}_1} - (K_2 - k_2')\, Z_2^2 - k_2'\, Z_2'^2 \leq -\overline{K} V_2 \tag{33}$$

where $\overline{K} = min\Big\{K_1, k_1', \{K_2 - k_2'\}, k_2'\Big\}$.

Finally, the control law inputs Γ_{em1}, Γ_{em2}, $\Delta\beta$ force respectively the angular velocities (Ω_1, Ω_2) and the yaw angle ψ to track their references;

$$\begin{cases} \Omega_{1,2} \longrightarrow \Omega^* = \dfrac{V\cos(\psi - \alpha)}{R}\, \lambda^{opt} \\ \psi \longrightarrow \psi^* = \alpha. \end{cases}$$

4. RESULTS AND DISCUSSION

In order to evaluate the performances of the control law, two permanent magnet synchronous generators ($2 \times 2MW$) are implemented in the model of TWT thanks to MATLAB/Simulink software. Parameters of the wind turbines can be found in [Uehara et al. (2011)]-[Guenoune et al. (2016)]. The proposed control strategy is compared to a proportional integral PI with several scenarios. The control parameters are given Table 1

IBC	PI
$K_1 = 3.5$, $k_1' = 0.01$	$K_{p\psi} = 15$, $K_{i\psi} = 0.8$
$K_2 = 0.3$, $k_2' = 0.001$	$K_{p\Omega i} = 2 \cdot \epsilon \cdot w_n \cdot J$, $K_{i\Omega i} = w_n^2 \cdot J$
$K_{\Omega i} = 5$, $k_{\Omega i}' = 0.001$	$\epsilon = 0.7$, $w_n = 1$

Table 1. IBC and PI parameters.

Case 1. The TWT is considered to be face the wind ($\alpha = 0$), and a variable wind speed profile is applied (Figure 4-left).
Note that for this case, only results of WT 1 are displayed, those obtained for WT 2 being similar.
Pitch angles and power coefficients are shown in Figure 4. It can be observed that the C_{p1} has a value close to its optimal value (0.4) and is not affected by the wind speed variation, when the TWT is controlled by the proposed strategy. In contrast, with PI controller, C_{p1} is around this optimal value. The time varying angular velocity is displayed in Figure 5-top. A good tracking for Ω_1 is obtained with the two controllers, but an overshoot is registered for PI. Figure 5-bottom shows the generated power by applying the proposed strategy.

Case 2. The wind direction varies according three values; $\alpha = 0°, 10°, 20°$, whereas the wind speed is supposed to be constant ($V = 11.5m/s$). The yaw angle, drag forces difference and pitch angles are displayed in Figure 6. It can be observed that the structure requires some time to be face the wind, due to the huge structure of SEREO system. The pitch angles are actuated to inducing drag forces difference (Figure 6 top-right) which rotates the structure. The power coefficient and the generated power are given in Figure 7. When the TWT operates in yaw mode, the power coefficients are degraded, because the pitch angles are modified (not formally optimal) to move the structure. Consequently, a power loss is got during the rotation. The loss of power with the PI controller is more important than with the proposed strategy (Figure 7-bottom).

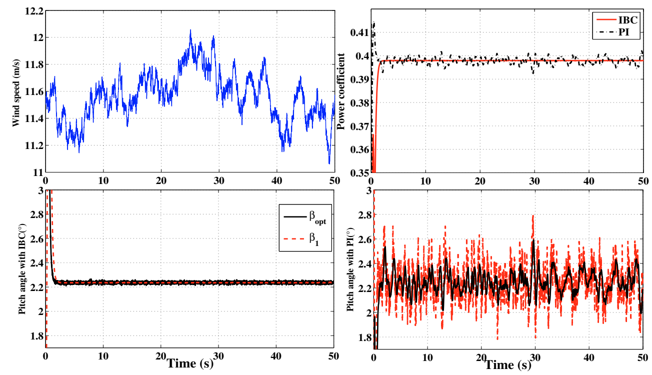

Fig. 4. Case 1- **Top-left** - Wind speed (m/s) versus time (sec). **Top-right** - Power coefficient (C_{p1}) versus time (sec). **Bottom-left** - Pitch angle β_1 (°) with IBC versus time (sec). **Bottom-right** - Pitch angle β_1 (°) with PI versus time (sec).

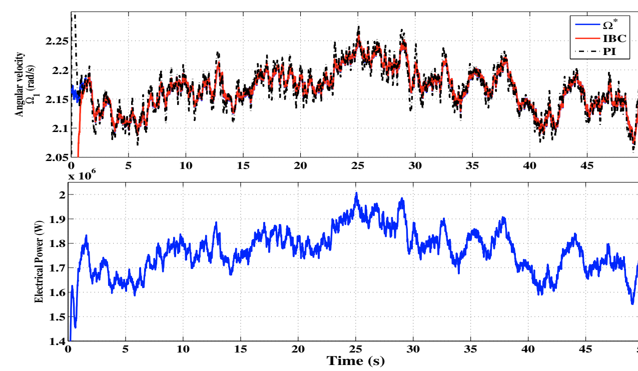

Fig. 5. Case 1 - **Top** - Angular velocity Ω_1 (rad/s) versus time (sec). **Bottom** - Electrical power (W) with IBC versus time (sec).

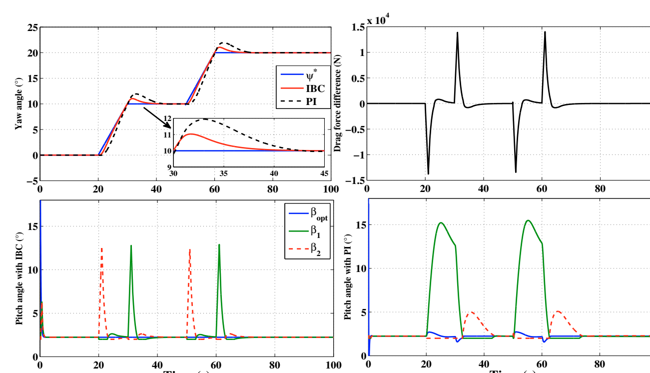

Fig. 6. Case 2 -**Top-left** - Yaw angle (°) versus time (sec). **Top-right** - Drag forces difference (N) versus time (sec). **Bottom-left** - Pitch angles β_i (°) with IBC versus time (sec). **Bottom-right** - Pitch angles β_i (°) with PI versus time (sec).

Case 3. The goal of this test is to check the effectiveness

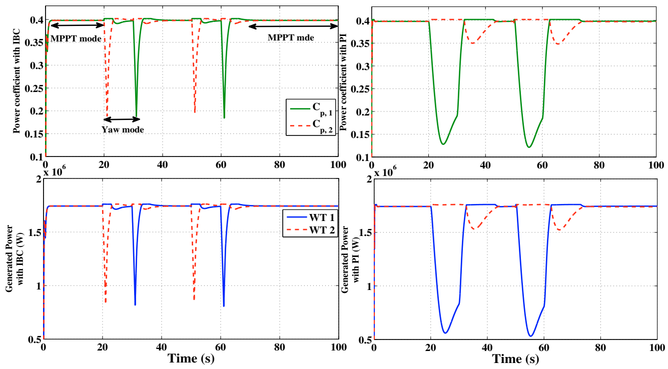

Fig. 7. Case 2 - **Top-left** - Power coefficient C_{pi} with IBC versus time (sec). **Top-right** - power coefficient with PI versus time. **Bottom-left** - Generated power (W) with IBC versus time (sec). **Bottom-right** - Generated power (W) with PI versus time (sec).

of the proposed strategy against the parameters uncertainties. A similar scenario as Scenario 2 is considered, but by supposing uncertainties on the drag forces F_{di} and aerodynamic torques Γ_{ai}. One assumes uncertainties of 15 % and 10% respectively between torques and drag forces appearing in the model. Similar results are close to those obtained previously with the integral backstepping strategy. With the standard PI, there is a modification in pitch angles, which deteriorates the power coefficient, *i.e.* energy producing (see Figure 8-bottom).

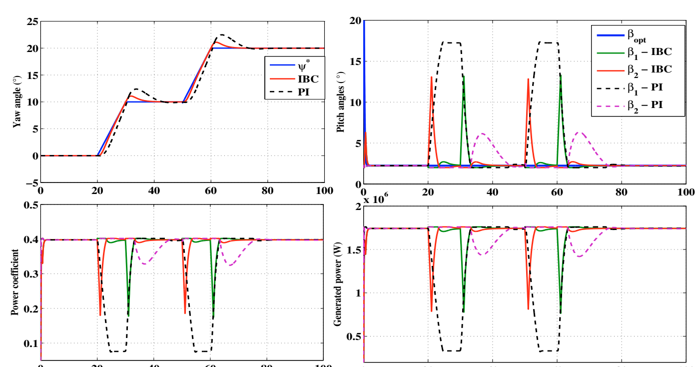

Fig. 8. Case 3 - **Top-left** - Yaw angle (°) versus time (sec). **Top-right** - Pitch angles β_i (°) versus time (sec). **Bottom-left** - Power coefficient C_{pi} versus time (sec). **Bottom-right** - Generated power (W) versus time (sec).

5. CONCLUSION AND FUTURE WORK

An integral backstepping controller applied on the new structure of the twin wind turbines has been presented in this work. The power optimization strategy is combined with a control of the yaw rotation to produce the maximum energy. The motion of the yaw angle is achieved without using an actuator, in contrast to standard wind turbine which uses a motor to rotate the nacelle. The control of the SEREO system includes two parts. The yaw angle is controlled, by acting on the drag forces difference, in order to keep the structure face the wind. The control of electrical part consists in controlling the angular velocities at their optimal values, and by adjusting the generators torques to get a larger value of power coefficient. The proposed control strategy guarantees the global asymptotic convergence of the system. Future works consist in

- establishing an other solution to rotate the twin wind turbines face the wind by controlling the output generator power of the two wind turbines;
- in comparing the gains of the SEREO structure with two standard wind turbines which are equipped with an actuator for nacelle system, in order to evaluate the power production in both modes, MPPT and yaw motion.

REFERENCES

Beltran, B., Ahmed-Ali, T., and Benbouzid, M. (2009). High-order sliding-mode control of variable-speed wind turbines. *IEEE Trans. Ind. Electronics.*, 56(9), pp. 3314–3321.

Georg., S., Schulte., H., and Aschemann, H. (2012). Control-oriented modelling of wind turbines using a takagi-sugeno model structure. In *International Conference on Fuzzy Systems*. Brisbane, Australia.

Glumineau, A. and d. L. Morales, J. (2015). *Sensorless AC Electric Motor Control Robust Advanced Design Techniques and Applications.* Springer International Publishing.

Guenoune, I., Plestan, F., and Chermitti, A. (2016). Control of a new structure of twin wind turbines. In *International Conference on Renewable Energy*. Birmingham, UK.

Herskovits, A., Laffitte, O., THOME, P., and TOBIE, A. (2014). V-shaped, bi-rotor wind generator on a spar floating structure.

Jafarnejadsani, H., Pieper, J., and Ehlers, J. (2013). Adaptive control of a variable-speed variable-pitch wind turbine using radial-basis function neural network. *IEEE Trans. Control Syst. Technology*, 21(6), pp. 2264–2272.

Mesemanolis, A. and Mademlis, C. (2014). Combined maximum power point and yaw control strategy for a horizontal axis wind turbine. In *International Conference on Electrical Machines*. Berlin, Germany.

Munteanu, I., Bratcu, A., Cutululis, N., and Emil, C. (2008). *Optimal Control of Wind Energy Systems.* Advances in Industrial Control, Springer.

Shariatpanah, H., Fadaeinedjad, R., and Rashidinejad, M. (2013). A new model for pmsg-based wind turbine with yaw control. *IEEE Trans. Energy Convers.*, 28(4), pp. 929–937.

Tang, C, Y., Guo, Y., and Jiang, J, N. (2011). Nonlinear dual-mode control of variable-speed wind turbines with doubly fed induction generators. *IEEE Trans. Control Syst. Technology*, 19(4), pp. 744–756.

Uehara, A., Pratap, A., Goya, T., Senjyu, T., Yona, A., Urasaki, N., and Funabashi, T. (2011). A coordinated control method to smooth wind power fluctuations of pmsg-based wecs. *IEEE Trans. Energy Convers.*, 26(2), pp. 550–558.